

mesago

**pcim**  
EUROPE

9 – 11.05.2023  
NUREMBERG

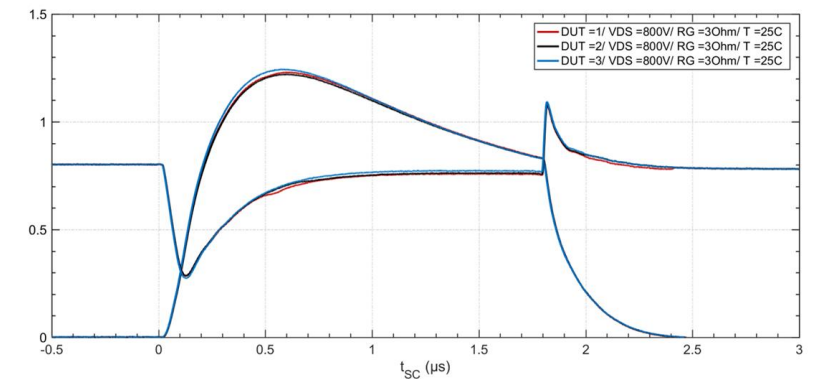
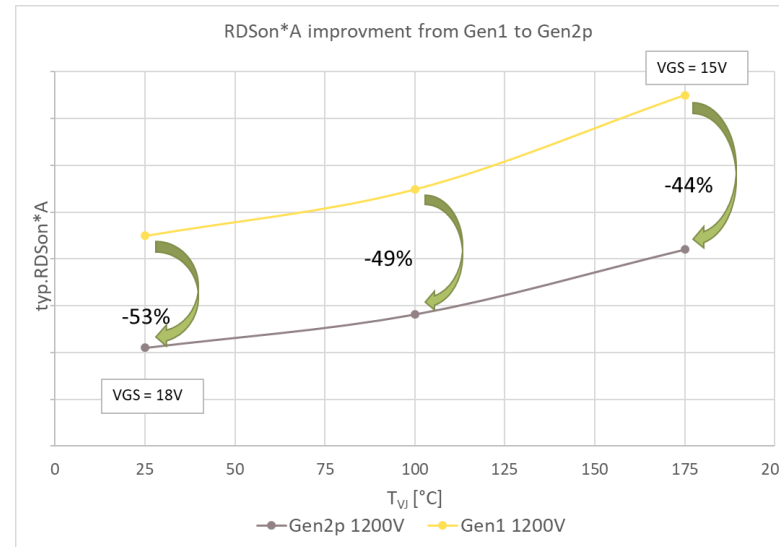
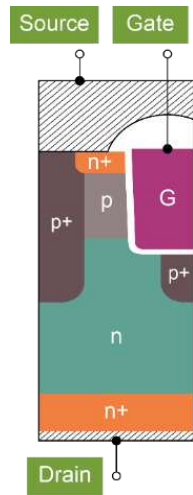
# Performance and Feature Benchmarking of SiC Trench Technologies and Cooling Systems for DSC Modules in Traction Inverters

Dustin Meichsner  
Product Manager  
Infineon Technologies AG

12 April 2023

Messe Frankfurt Group

# 1200 V CoolSiC™ Gen2p High Performance SiC Trench Technology for Inverter



Automotive proven Gen1 trench cell concept further improved by multiple measures, e.g. EPI drift zone optimization.

Significant RDSON\*A benefit achieved, reducing dominant loss contribution during inverter operation.

Necessary short-circuit robustness provided.

**The 1200 V CoolSiC™ Gen2p with optimized trench concept enables higher range for inverter systems in conjunction with necessary robustness due to further improved efficiency.**

# Infineon's SiC optimized DSC Power Module

## High scalability in a small footprint

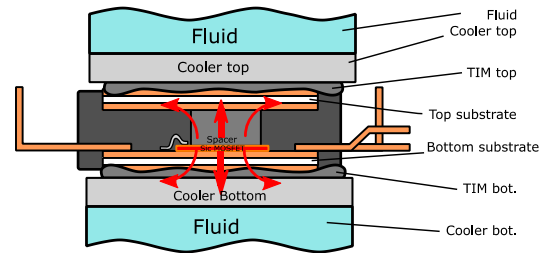


### Double Sided Cooled Power Module



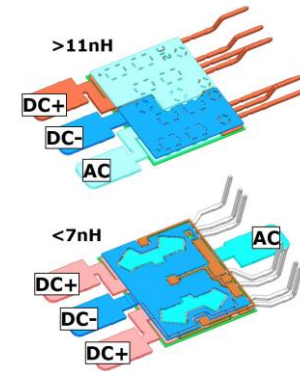
- High efficiency
- High power density
- High Scalability
  - V: [650 ;1200]
  - $A_{RMS}$  [100,450]

### Thermal Stack



- Dual cooling path
- Up to 40% lower  $R_{th,jf}$  than single cooling path
- Heat dissipation split about 30% top and 70% bottom
- Indirectly cooled
- TIM between package and cooler

### Optimized Electrical Layout



- Low stray inductances <7 nH
- Optimized for low  $R_{DS(on)}$  due to high symmetry of electrical layout

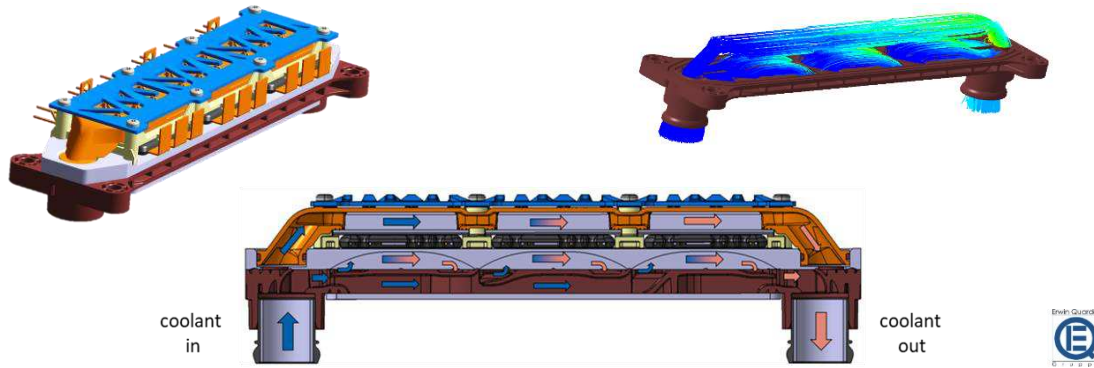
The updated SiC-specific design caters to applications requiring high power density and efficiency. The low  $R_{DS(on)}$  and stray inductances further support the benefits of the SiC Trench MOSFET technology.



# Benchmarking of two DSC-tailored coolers

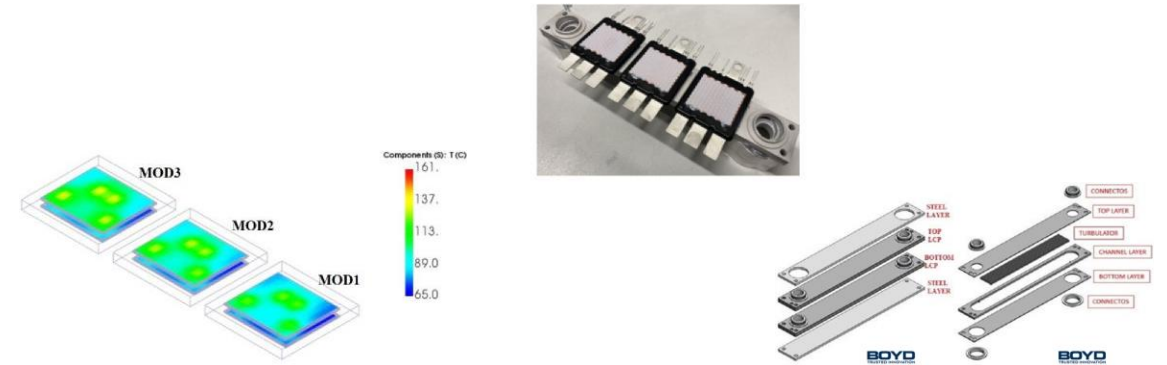
## High performance focus with different trade offs

### Hybrid Cooler



- 3\* DSC Halfbridges positioned by support frame and clamped with ~800 N in-between top/bottom cooler
- Hybrid Cooler with Plastic / Aluminium configuration
- Serial cooling on top side and parallel cooling on bottom side
- Top cooler flexible: adaptation to Hight- and co-planarity tolerances as well as thermo-mechanical deformation

### Aluminium-Sheet Cooler



- Extremely low volume profile for space sensitive applications
- Low Design complexity with high quality materials designed for robustness
- Controlled Atmosphere Brazing (CAB) process, a metallurgic welding process allowing for a high-quality metal junction
- Turbulators designed inside of the Liquid cooling plates for improved heat transfer

**Both coolers are designed for high-performance. They set different design targets for complementary dimensions, such as reliability, size, ease of design and assembly and cost.**

# Cooler System Level Benchmarking

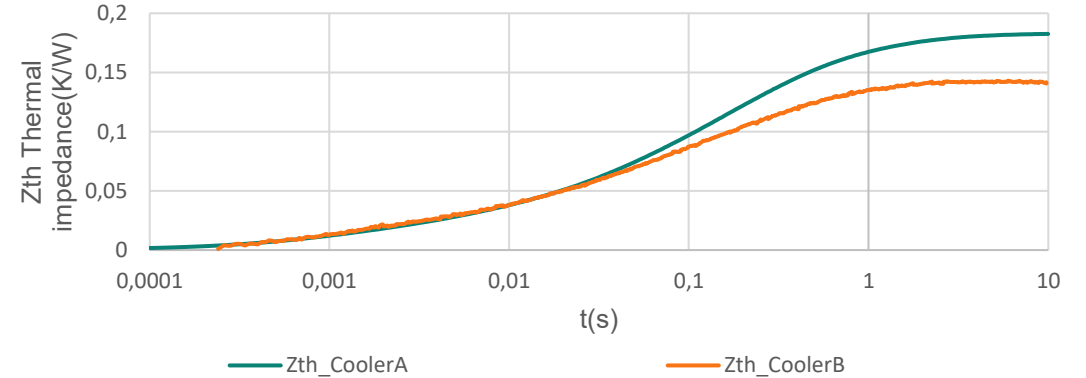
## Performance and additional selection criteria

### Benchmark Overview

Parameters	Units	Cooler A	Cooler B
Dimensions (L x W x H)	[cm <sup>3</sup> ]	21 x 2.83 x 6.81 =0.4L	21.1 x 6.9 x 5.6 =0.81L
Material		Aluminum	Plastic Aluminum
Feature set		Folded fins	Thin fins/ springs
Weight	[g]	560	540
Pressure drop	[mBar]	200	49.7
Rthj-f	[K/W]	0.183	0.141

- Cooler A well suited for highly space-restricted applications with only 0.4 Liters, hence 50% of the volume occupied by Cooler B
- Despite difference in volume, both cooler of similar weight due to use of plastic in Cooler B
- Pressure Drop of Cooler B significantly lower (25% of Cooler A)
- Both Coolers with good Rth,jf values with Cooler B being relatively better by averaged 0.04 K/W

### Thermal Impedance



- Both cooler systems were equipped with three equal DSC power modules
- One DSC half-bridge module consist of two switches and 96 mm<sup>2</sup> SiC chip content – Gen2P 1200 V technology
- Clamping force of 800 N is applied to each module. A thermal paste of 6 W/mK and around 50 μm thickness is applied
- Both coolers were tested with a water pressure of 1 Bar at an inlet temperature of 65°C

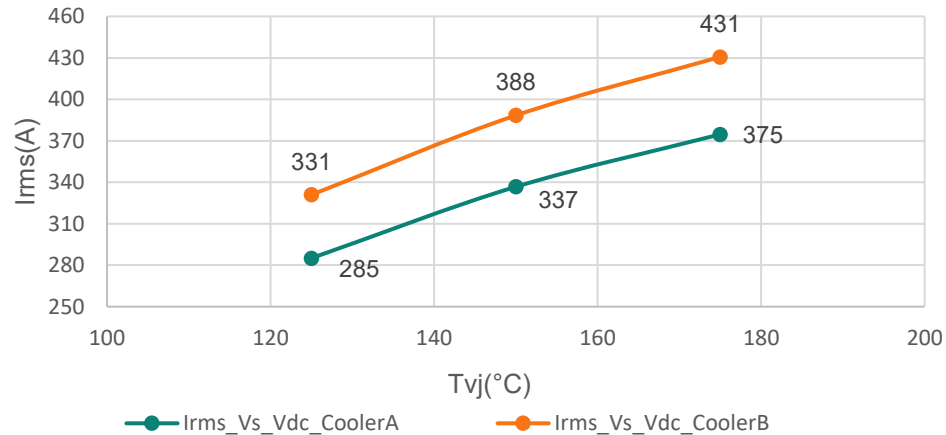
**Both Cooler A and B can satisfy customers key design parameters between volume, performance and costs. Cooler A is more suitable for low profile main inverters whereas Cooler B is more performance focused.**

# Inverter Performance Benchmarking

## Current per phase comparisons as a function of $T_{vj}$ and $V_{dc}$

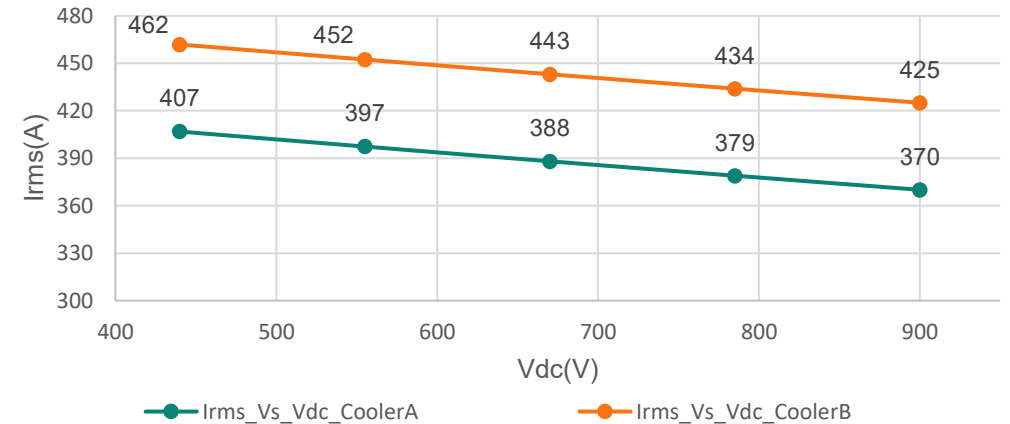


### RMS Current as function of $T_{vj}$



- Simulated DSC power modules in an inverter configuration with two different cooling systems
- DC voltage applied was 850 V, switching frequency 10 kHz, modulation index 0.9, and power factor 1
- Cooler B offers better overall Irms current of the inverter compared with Cooler A due to more efficient heat dissipation (4200 W vs 3500 W)

### RMS Current as function of Battery Voltage



- Performed another simulation to get a current projection for different battery voltages at  $T_{vj}$  175 °C by varying the DC
- For the 450 V system, a current of 400 to 450 A can be reached depending on the cooling system applied
- Inverter using these voltages and frequencies could then reach a power of 350 kW using DSC Modules installed in Cooler B and 310 kW when installed in Cooler A

**Lower thermal resistivity is directly translated into higher current capability.  
With a voltage of 850 V at 10 kHz and a  $T_{vj}$ =175°C, the Infineon DSC module can reach up to >400 Arms.**

# System Cost Benchmarking

## A general approach to understand potential commercial impacts



	Chip size reduction	FE cost-share	BE cost-share	Package cost savings
Scen.1	10%	30%	70%	3%
Scen.2		50%	50%	5%
Scen.3		70%	30%	7%

	Package cost savings Case A	Package cost savings Case B
Scenario 1	9 €	6 €
Scenario 2	15 €	11 €
Scenario 3	21 €	15 €

### Assumptions Mapping

- Poweroutput for both systems (cooler + power module) equal
- Relative Rthjf advantages on cooler level are used to reduce performance of power module by chip-size reduction
- 10% chip-size reduction (based on simulation)
- Three cost-structures assumed (see Table 1)
- Linear relationship between chip-size and cost. Hence, 10% size reduction results in 10% cost reduction
- Package Cost assumption for Case A 100 Euro/pc and 70 Euro/pc for Case B

### Not taken into account

- Reliability, ease of high-volume assembly, design complexity and non-linearities

**Investing in higher performing cooler solutions can pay off on system level. The method should be used to further the system cost discussion by adding components and cost drivers and advancing on the assumptions side.**

# Summary and outlook



- The paper discussed different design objectives for power modules and cooler-systems used in three-phase, water-cooled traction inverters of electric vehicles.
- On the Front End Technology side, we analyzed that 1200 V CoolSiC™ Gen2p with optimized trench concept enables higher range for inverter systems in conjunction with necessary robustness.
- Two DSC-specific high-performance coolers with different design concepts, performance attributes, maturity stages, and costs were benchmarked.
- While both showed high performance in terms of thermal management, one was more optimized towards total  $R_{th}$  reduction, while the other was optimized for applications demanding a low-volume solution.
- Investing in higher performing cooler solutions can pay off on system level. The method should be used to further the system cost discussion by adding components and cost drivers and advancing on the assumptions side.



mesago

**pcim**  
EUROPE

9 – 11.05.2023  
NUREMBERG

# Thank you for the attention!

I'm pleased to answer your questions.  
[dustin.meichsner@infineon.com](mailto:dustin.meichsner@infineon.com)

# Performance and Feature Benchmarking of SiC Trench Technologies and Cooling Systems for DSC Modules in Traction Inverters

Dustin Meichsner<sup>1</sup>, Anthony Thomas<sup>1</sup>, Ben Rosam<sup>1</sup>, Christian Schweikert<sup>1</sup>, Matias Leitner<sup>1</sup>

<sup>1</sup> Infineon Technologies AG, Germany

Corresponding author: Dustin Meichsner, Dustin.Meichsner@infineon.com

Speaker: Dustin Meichsner, Dustin.Meichsner@infineon.com

## Abstract

This paper explores a relevant subset of the trade-offs involved in selecting power modules for traction inverters of electric vehicle drivetrains. The discussion proceeds with the example of two Silicon Carbide (SiC) MOSFET generations, the Double Side Cooled (DSC) frameless molded power module, and two DSC-specific cooler systems. Conflicting objectives such as product performance, system performance, ease of integration, and low costs demand a differentiated analysis of product features and their benefits. Hence, we discuss the impact of SiC Generation 1 and tailored SiC Generation 2 "Performance" on inverter efficiency and performance, followed by a comparison of two high-performance cooling systems using three DSC power modules. Finally, we examine potential system cost implications that can inform the selection of an appropriate cooler system for a given application. The paper is part of a three-publication series, with the previous two focusing on technical details for both cooling systems.

## 1 General motivation

When choosing the best power module for given application requirements, solely considering the module's performance is insufficient. It is essential to consider trade-offs between objectives, such as cost versus performance, and the interrelationships between components, including the power module and cooler. Therefore, a system-level analysis and clear assumptions mapping are necessary. This paper examines the implications of three traction inverter components (chip, power module, cooler) on performance, both at the component and system level, and on system cost, which are two critical trade-offs to consider.

## 2 Introduction of the Silicon Carbide MOSFET technology

With its novel automotive 1200V CoolSiC™ Gen2p high performance SiC trench technology, Infineon has tailored its technology specifically to the requirements of the inverter application for electric cars. It provides pronounced improvements which can be converted into significant higher current output power capability for 800V battery systems.

The DSC module specifically levers the performance to its best.

The Gen2p technology is based on a Gen1 trench transistor cell concept (see Fig. 1), which has been proven to provide an excellent  $R_{DS(on)} \cdot A$  and switching performance, such as high controllability of switching, and minor switching losses being key features [1], [2], [3]. With Gen2p, the trench technology has been further optimized to provide best performance for inverter applications. To enable a significantly lower area-specific  $R_{DS(on)}$ , the cell pitch has been reduced in order to increase the channel density. The EPI drift zone region depth was reduced to adjust VBR margin to stray inductance of newest generation of power

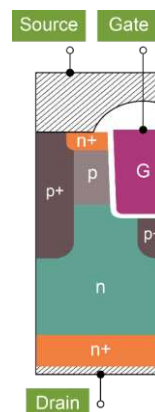
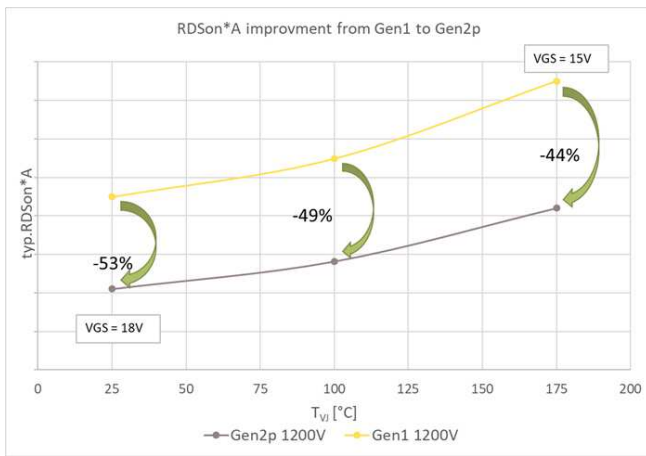


Fig. 1 CoolSiC™ MOSFET cell structure.

modules without compromising cosmic ray robustness. In addition, the cell design and the process have been optimized. Fig. 2 shows the relative static loss benefit between the two generations over temperature.



**Fig. 2** Typical RDson\*A performance comparison as function of chip temperature, with ~ 50% benefit across the whole temperature region.

The CoolSiC™ trench technology provides lower channel resistance than commercial DMOS-cell-based SiC MOSFETs. Improvements of the MOS system enabled us to use a higher on-state gate voltage of 18V at constant gate oxide reliability. Subsequently, also the RDson is lower even at high temperatures, and the share of total on-resistance is smaller for the channel in general. The temperature-behaviour is more dominated by the drift zone. The positive  $T_k$  provides an extra low static loss at light load condition, the predominant driving condition and thus enables high efficiency, which is a prime design target for the inverter system. Latter reduces the battery capacity and hence costs for a targeted (e.g. WLTP) driving range. Additionally, a positive and higher  $T_k$  favours a robust current balancing for multi-chip designs in power modules, which is the typical use case.

The substantially improved loss performance is paired with the necessary short circuit robustness, a key requirement for traction inverter systems. Fig. 3 provides representative short-circuit curves of repeated tests using a randomly selected sample. The Gen2p CoolSiC™ technology provides a robustness allowing repeated short-circuit events.

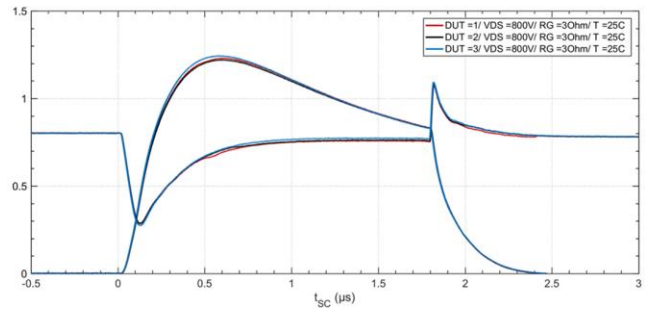


**Fig. 3** Typical short-circuit characteristic and reproducibility of a representative SiC Gen2p chip.

### 3 DSC power module technology

To achieve a high-performance power module, both chip and package technology must be optimized. Important aspects to consider on the package side include the thermal stack, as well as parasitics resulting from topology and commutation loops, such as internal symmetry and power scalability of the module. This sub-chapter introduces the DSC package, which contains a SiC Trench MOSFET chip technology inside.

#### 3.1 Thermal stack and inner structure

The internal structure of a DSC module is shown in Fig. 4. The performance and reliability of the package heavily rely on the materials used for the insulation layer (substrate) and interconnection technologies employed for the respective interfaces. One of the unique features of the DSC is the presence of an electrically and thermally conductive spacer along with a mold compound, which is a polymer-based material designed to provide electrical insulation while withstanding the mechanical and thermal stresses generated during application.

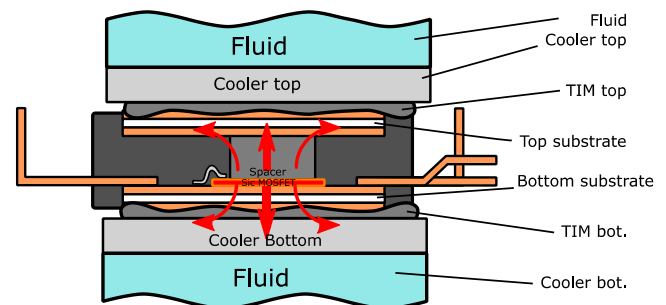


**Fig. 4** DSC thermal stack and heat dissipation channel.

The use of two cooling paths reduces the thermal resistance ( $R_{th,jf}$ ) between chip and fluid by up to



40% compared with the traditional single-side cooling methodology with equal die content (see [4]). The heat dissipation split in the package is about 30% to the top and 70% to the bottom. This is a consequence of the thermal stack (including the spacers) and the closer proximity of the heat source (chip) to the bottom of the package. The DSC is indirectly cooled by the cooling system by at least one layer between either side of the package and fluid - typically a 50/50% water-glycolic mixture. A thermal interface material (TIM) or so-called thermal grease is applied between the package and the cooler. It is important to mention that the TIM paste plays an important role in the dissipation of the package's heat. The better the thermal conductivity of the thermal paste, the lower the thermal resistivity of the package will be. Graphite foils are an alternative to TIM paste.

### 3.2 Electrical layout and stray inductance

Design optimization of the DSC package for SiC resulted in improved performance and reliability [4]. DC power tabs and substrate layout have been modified to enable lower stray inductances targeting the value of 7 nH. Other measures for decreasing the RDSon include a highly symmetrical layout of resistances and inductances in both the control and power loops to ensure equal current sharing between the chips, prevent inter-chip oscillations, and improve switching control even under short circuit conditions. The module is designed with a negative feedback loop through the introduction of common-source inductance to balance the switching current during turn-on and turn-off. Moreover, the gate connection is designed to be symmetrical

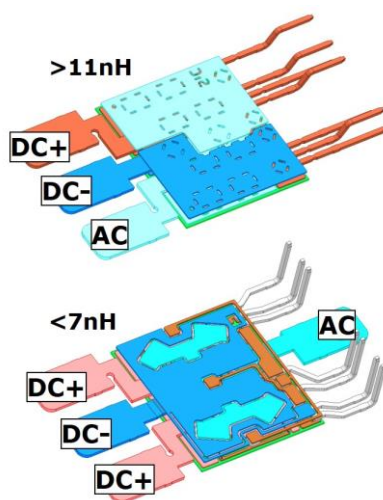


**Fig. 5** DSC layout optimization for improved stray inductance [4].

for each die of a switch. The global stray inductance layout comparison between two and three DC power tabs can be found in Fig. 5.

### 3.3 System level consideration – scalability and flexible mechanical integration

In designing the package, various trade-offs need to be considered, such as the thermal conductivity of each layer, as well as electrical, thermo-mechanical, and commercial considerations. Based on the half-bridge design, the DSC enables flexibility in inverter design for size and weight-sensitive applications, furthermore allowing for output scalability at a constant footprint, ranging from 650 V to 1200 V and from 100 up to 450 ARMS.

## 4 Cooling systems for DSC power modules

This benchmark compares two high performance DSC coolers. A) an aluminum sheet cooler from Boyd Corporation and B) a hybrid cooler system from Erwin Quarder Group. We start by shortly describing both systems and their production processes. Detailed explanations of the respective benefits can be found in [5] and [6].

### 4.1 Aluminum cooling system from Boyd

#### 4.1.1 Cooler topology

The aluminum-based Boyd cooler for DSC power modules, aimed at achieving a high-power density in a compact form factor, can be seen in Fig. 6. The cooling system employs two identical Liquid Cold Plates (LCPs).

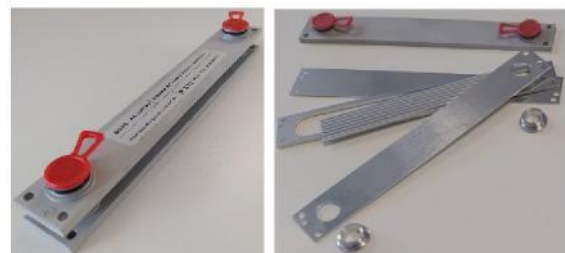


**Fig. 6** Fabricated Boyd cooler [5].

The LCPs share the same geometry in terms of the number of layers, inlet/outlet connectors, channel structure, turbulator, and perimeter shape. Each LCP comprises a top layer with inlet/outlet hydraulic connectors, a channel layer with a turbulator, and a bottom layer to seal the channel path. The top LCP features two additional hydraulic connectors to evenly distribute the fluid

flow rate between the top and bottom. The interfaces between the LCPs are sealed with O-rings. The layers are laser cut, connectors are lathe-made, and turbulators are stamped. To compensate for any warpage effect that might reduce the contact surface between the LCPs and the central SiC module during assembly, two steel plates are added on top and bottom. Cooling structure and DSC modules combined occupy a volume of only 0.4 L, which paves the way for high-power density.

#### 4.1.2 Production process for metal sheet cooler

The liquid cold plates are manufactured using the Controlled Atmosphere Brazing (CAB) process (see Fig. 7) resulting in a high-quality metal junction. During the assembling process, foils of filler material - made from a specific aluminum mixture - are placed between the aluminum layers. The structure is clamped and processed in an oven under a nitrogen atmosphere to avoid oxidation. Once the oven reaches an internal temperature of approximately 600°C, the foil material starts melting while the aluminum layers are still in a solid stage. After cooling, the pieces are gradually cooled down to ambient temperature. The specific combination of aluminum alloy used in the CAB brazing process is crucial to avoid micro-porosities along the brazing junction, which could cause leakage and lead to LCP failure during operation.

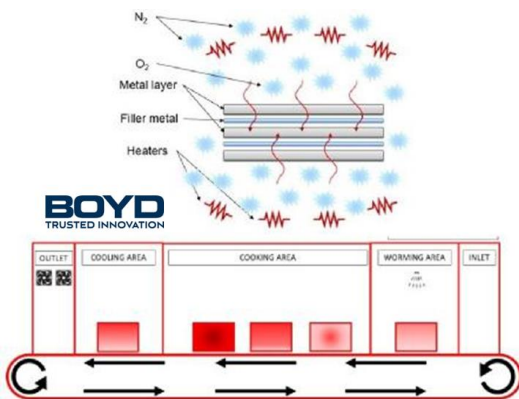


Fig. 7 CAB Brazing process [5].

## 4.2 Plastic-aluminum hybrid cooling system from Quarder

### 4.2.1 Cooler topology

Quarder's plastic-aluminum cooling system (see Fig. 8) consists of a bottom and a top cooler. The top cooler includes three aluminum blocks with a nanostructure fin-topology and cools the three DSC modules sequentially. The bottom cooler uses parallel cooling of all DSCs. Based on the

heat dissipation ratio for DSC modules, the coolant is divided in a 20/80 ratio between top and bottom, and the volume flow of the bottom cooler increases slightly from the first to the last module to compensate for the thermal gradient in the top cooler. The surfaces have low roughness and flatness for good contact. Flexible joints and metal springs compensate for mechanical tolerances and thermo-mechanical phenomena. A thermal interface material is applied to both sides of the module.

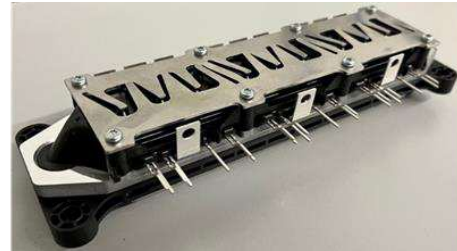


Fig. 8 Quarder cooler concept with parallel (top) and sequential cooling (bottom) [6].

### 4.2.2 Production process

The hybrid cooler utilizes an innovative joining technology resulting in a robust bond between aluminum and plastic (see Fig. 9 Fig. 9).

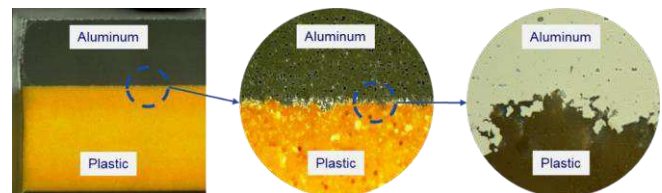


Fig. 9 Cross section of mechanical connection of aluminum and plastic [6].

The connection is media-tight, eliminating the need for additives such as adhesives or seals. To achieve this, the surface of the aluminum is structured through a nanoscale sculpturing process, creating undercuts, ditches, and caves that increase the surface area significantly. During the joining process, the aluminum is heated to the melting temperature of the polymer, and the plastic component is pressed onto the structured surface, allowing the polymer to melt and penetrate the surface.

This joining process occurs under non-specific environmental conditions, eliminating the need for a vacuum or inert gas atmosphere. After cooling, a mechanical and media-tight connection is formed between the aluminum and plastic without voids.



### 4.3 Cooler benchmarking

Boyd's metal sheet cooler (Cooler A) and Quarder's plastic-aluminum cooler (Cooler B) have been benchmarked in terms of volume, features, and pressure drop along with thermal resistance performance. A summary of the cooler benchmarking can be found in Table 1. The dimensions of cooler A are about 40% than cooler B. Thanks to its construction - using thin aluminum metal sheets – Cooler A is more suitable for applications requiring a compact integration.

Parameters	Units	Cooler A	Cooler B
Dimensions (L x W x H)	[cm <sup>3</sup> ]	21 x 2.83 x 6.81	21.1 x 6.9 x 5.6
Material		Aluminum	Plastic Aluminum
Feature set		Folded fins	Thin fins/springs
Weight	[g]		
Pressure drop	[mBar]	200	49.7
R <sub>thj-f</sub>	[K/W]	0.19	0.141

**Table 1** Benchmark values for investigated cooler system properties.

To assess the thermal resistance of both systems between junction and fluid and to evaluate the pressure drop, both cooler systems were equipped with three equal DSC power modules for a three-phase traction inverter configuration. One DSC half-bridge module consist of two switches and 96 mm<sup>2</sup> SiC chip content - Gen2P 1200V technology. The modules are placed within the cooling plates and a force of 800 N is applied to each module. A thermal paste of 6 W/mK and around 50 μm thickness is applied. As mentioned previously, it is important to use TIM to improve the thermal conductivity of the interface between DSC and cooler. Neglecting this step would have an impact on the global thermal performance of the cooler.

Both Coolers were tested with a water pressure of 1 Bar at an inlet temperature of 65°C. The pressure loss for Cooler B is lower, with pressure loss of 200 mBar Cooler A versus 49.7 mBar Cooler B. A potential reason is the different approach to the turbulator structure. Cooler B has a higher number of fins with a thinner structure. Hence, the resistivity of the water flow is reduced, resulting in lower pressure losses.

Fig. 10 compares the thermal impedance between junction and fluid ( $Z_{th,jf}$ ) of the two systems. The values are measured and averaged per switch. To characterize such a parameter, a pulse current is biased into the three DSC modules to provoke the maximum virtual junction temperature ( $T_{vj}$ ) of the

modules, here 175°C. A pre-calibration is necessary to correlate the needed voltage with the respective junction temperature of each switch.

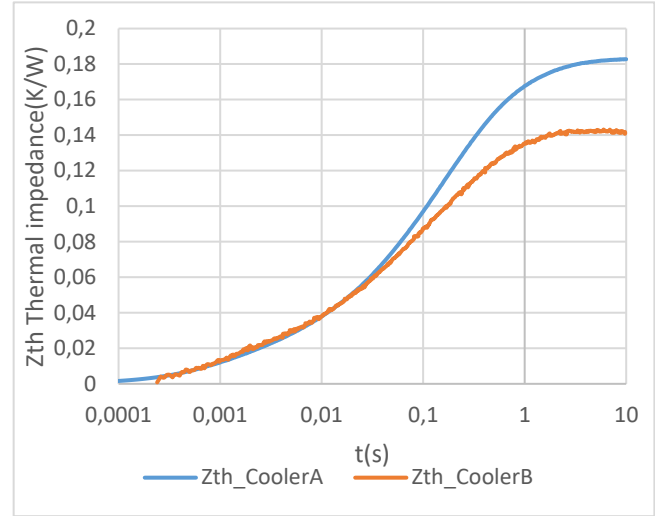


**Fig. 10** Thermal impedance benchmark between Cooler A and Cooler B.

Such a characterization is realized using the body-diode voltage based on Jedec standard [JESD24-12]. The high-pulsed current provokes the heating of the chip until the maximum  $T_{vj}$  is reached with the MOSFET in on-mode. During this phase, the current flowing into the MOSFET channel, generating the power loss. Right after the current pulse is stopped, a marginal current – roughly 1000 times lower than the high-pulsed current - is injected into the diode to determine the switch's temperature. During the characterization, the cooler inlet and outlet temperatures are monitored. The global  $R_{th,jf}$  then can be calculated with Eq. (1).

$$Z_{th,j-f}(\infty) = R_{th,j-f} = \frac{T_{vj} - (T_{cool,in} + T_{cool,out})/2}{P_{loss\_switch}} \quad (1)$$

Please note that the resulting average  $R_{th,jf}$  is per switch but depends on the global system performance. When three DSC modules are placed in a row and sequential cooling is applied, the water inside the cooler gradually warms up from one to the other module. This leads to a relatively worse thermal resistance compared to single DSC mode, which is prescribed in the AQG324 V3.1. However, the three-switch characterization is much closer to real applications.

Comparing the  $R_{th,jf}$  performance of both cooling systems, it can be seen that a  $R_{th,jf}$  per switch is reaching 0.14 K/W for Cooler B and 0.18 K/W for Cooler A.

## 5 Inverter performance benchmark of today's cooler

For an inverter level comparison, the DSC power modules have been simulated in an inverter configuration given the respective  $R_{th,jf}$  values for the two cooling systems. The DC voltage applied to the modules was 850 V, the switching frequency 10 kHz, the modulation index 0.9 and the power factor 1. The biasing resistor value for switching the modules in on and off mode is 5.1Ω. The available RMS current per phase of the inverter versus max  $T_{vj}$  is depicted in Fig. 11.

It can be observed that Cooler B offers better overall  $I_{rms}$  current of the inverter compared with Cooler A due to more efficient heat dissipation. The resulting heat dissipation is 4200 W for the three DSC power module solution using Cooler B and 3500 W using Cooler A.

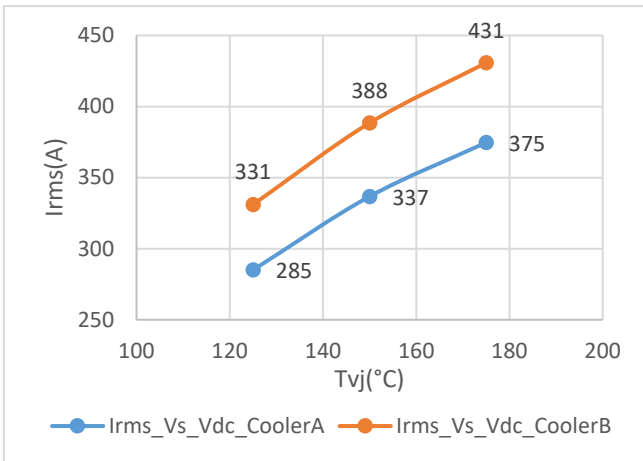


**Fig. 11** Available RMS current per phase of the modules vs. max junction temperature using cooler A and cooler B.

Another simulation has been performed to get a current projection for different battery voltages at  $T_{vj}$  175 °C by varying the DC. The comparison can be found in Fig. 12. For the 450 V - relatively lower battery voltage - system, a current of 400 to 450 A can be reached depending on the cooling system applied. An inverter using these voltages and frequencies could then reach a power of 350 kW using DSC Modules installed in Cooler B and 310 kW when installed in Cooler A.

As power output requirements for applications are usually fixed, the benefit of a higher output system might not be needed. In this case, the power output could be kept constant and relative advantages in performance could be used to reduce the power output requirements on DSC module level. Based on our simulations, we could achieve this with a roughly 10% reduced chip size.

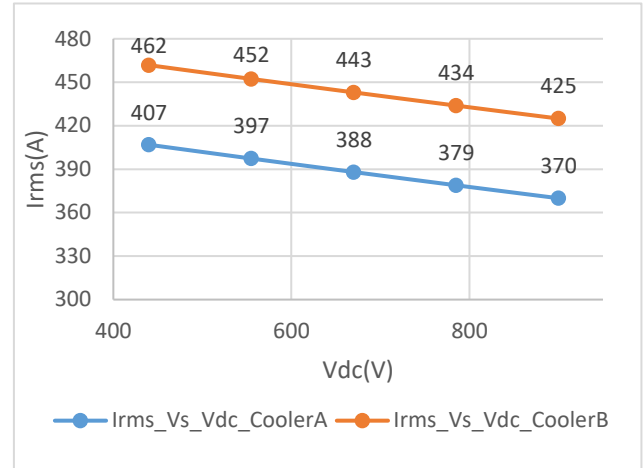


**Fig. 12** Current capability of the inverter vs. DC voltage for Cooler A and Cooler B.

## 6 System cost benchmark

In chapter 4.3 and 5 we discussed the performance of the two cooler-systems on product and system level respectively. We have found that both solutions are highly effective at dissipating heat and maintaining optimal temperatures for package and chip compared to industry standards.

Inverter design underlies diverse, and frequently conflicting design goals. Hence in this chapter we want to complement the before mentioned technical considerations with a system cost assessment. It is important to note that calculating system costs for power electronics is complex. The many existing intercorrelations, cause-and-effect relationships, and uncertainties result in second- and third-round effects. Hence, an exhaustive requirement and assumptions mapping would be needed for any given mission profile to make a reliable assessment.

Albeit, the following analysis is a starting point for more detailed investigations. We hope that this analysis will result in further explorations and fruitful discussions.

For this paper, we define system cost as the combined cost for three DSC half-bridges plus cooler-system. For a first approximation, we keep the power output of the two discussed systems equal and use relative performance advantages on cooler level to reduce performance on DSC package-level. Hence, we need to calculate how much SiC content can be saved, when applying the DSC modules in the cooler-system with a lower  $R_{th,jf}$ . Based on our simulations, we can shrink the SiC content by roughly 10% due to the better  $R_{th,jf}$ .

With this, let us now calculate potential cost impacts. To reflect different customer settings and applications, we define three scenarios reflecting three different cost structures. Scenario 1 reflects a cost structure in which 30% of the power module costs are attributed to the chip (Front End) and 70% to the package (Back End). Scenario 3 is the inverse case. In Scenario 2, Front End and Back End account equally to half of the total DSC module costs.

One important assumption concerns the impact of chip size reduction on cost. For simplicity, we assume a linear relationship between cost and chip size. Hence, a 18 mm<sup>2</sup> chip would cost 10% less, than a 20 mm<sup>2</sup> chip. Table 2 summarizes the discussed assumptions and their impact on package cost savings.

	Chip size reduction	FE cost-share	Be cost-share	Package cost savings
Scen.1	10%	30%	70%	3%
Scen.2		50%	50%	5%
Scen.3		70%	30%	7%

**Table 2** Package cost savings per scenario.

Based on the discussed assumptions and cost structures, savings on package-level between three to seven percent are possible, given the 10% chip size reduction due to the better  $R_{th,jf}$ .

For a simplified system cost assessment, the cost savings on package level must be offset by the relative cost increases on cooler level. Significant aspects, such as reliability, ease of high-volume assembly, design complexity and non-linearities are explicitly not taken into account.

Let us now discuss an application-near example with absolute, albeit assumed cost. Case A reflects a high-power application, while a relatively lower power application is accounted for by Case B. The assumed cost of one DSC half-bridge module is 100 Euro for Case A and 70 Euro for Case B. On total package cost level for a three-phase traction inverter, this computes to 300 and 210 Euro respectively. With the respective package cost savings shown in Table 2, the case and scenario-dependent package cost savings compute to six to twenty-one Euro (see Table 3). Or in other words, depending on the cost-structure and the power needs, savings between six to twenty-one Euro are feasible, given the mentioned simplifications and assumptions. Given a high-power application and a balanced cost-structure, the more performant cooler must be less than 15 Euro more expensive to realize system cost savings.

	Package cost savings Case A	Package cost savings Case B
Scenario 1	9 €	6 €
Scenario 2	15 €	11 €
Scenario 3	21 €	15 €

**Table 3** Absolute package cost savings per Case.

Finally, we want to stress again that the focus should be on the method and the discussed assumptions, not on the output. The many uncertainties, assumptions and higher-degree interdependencies prevent accurate results.

## 7 Conclusion

In this paper, we have discussed different design objectives for power modules and cooler-systems used in three phase, water-cooled traction inverters of electric vehicles. We have used a comparison of SiC Gen 1 and SiC Gen 2p to discuss performance implications from technology choices on product level. We have then benchmarked two DSC-specific high-performance coolers with different design concepts, performance attributes, maturity stages and costs. We showed that both coolers have benchmark  $R_{th,jf}$  performances compared to industry standards with the best value reaching an  $R_{th,jf}$  of as low as 0,14 K/W. We continued by discussing the relevant impact on the inverter level and found that an output gain of around 10% can be realized, due to the different thermal resistances. Finally, we discussed that system cost considerations are complex and depend on various factors. However, overall, we made the case, that investing in more performant coolers – which both of them are, relative to industry standards - can result in cost savings on the system level. We caution that this is a simplification. Ultimately, the decision to invest in a higher-performing cooler depends on a thorough analysis of the specific restrictions, application requirements, and mission profile and would need to include assembly cost, reliability, and durability factors as well as non-linearities and capacity impacts. As discussed in [6], the relatively higher-performing cooler is a concept and still has to undergo relevant qualifications.

## 8 Acknowledgements

The authors are thankful for the contribution of the companies Boyd and Erwin Quarder as well as for the targeted design of their coolers for DSC modules.

## 9 References

- [1] D. Peters, R. Siemieniec, T. Aichinger, T. Basler, R. Esteve, W. Bergner and D. Kueck, "Performance and ruggedness of 1200V SiC—Trench—MOSFET," in 2017 29th International Symposium on Power Semiconductor Devices and IC's (ISPSD), 2017.
- [2] P. Sochor, A. Huerner, Q. Sun, R. Elpelt, "Understanding the Switching Behavior of Fast SiC MOSFETs" in PCIM Europe 2022, Nuremberg, 2022
- [3] P. Sochor, A. Huerner, M. Hell, R. Elpelt, "Understanding the Turn-off Behavior of SiC MOSFET Body Diodes in Fast Switching Applications" in PCIM Europe digital days 2021
- [4] A. P. Pai, A. M.Ebli, T. Simmet, A. Lis and M. Beninger, "Characteristics of a SiC MOSFET-based Double Side Cooled High Performance Power Module for Automotive Traction Inverter Applications" 2022 IEEE Transportation Electrification Conference & Expo (ITEC)
- [5] A. P. Pai, A.Wihalm, M.Eibli, M.Kurz, M.Foresta, M. Osorio, "SiC MOSFET-Based High Performance Double Side Cooled Module and Compact Cooler for High Power-Density Automotive Inverter Applications " IWIPP 2021
- [6] Ch. Schweikert, S. Bruns, D. Meichsner „Enhanced performance and easy-to-integrate of double side cooled automotive power modules enabled by sophisticated cooling system" in PCIM 2023, International Exhibition and Conference for Power Electronics, Intelligent Motion, Renewable Energy and Energy Management